SOUTHAMPTON OCEANOGRAPHY CENTRE

INTERNAL DOCUMENT No. 66

Airflow distortion at instrument sites on the RV *Ronald H. Brown*

B I Moat, D I Berry & Yelland, M.J.

2001

James Rennell Division for Ocean Circulation and Climate
Southampton Oceanography Centre
University of Southampton
Waterfront Campus
European Way
Southampton
Hants SO14 3ZH
UK

Tel: +44 (0)023 8059 6406
Fax: +44 (0)023 8059 6204
Email: Ben.Moat@soc.soton.ac.uk

DOCUMENT DATA SHEET

AUTHOR

MOAT, B I, BERRY, D I & YELLAND, M J

PUBLICATION DATE
2001

TITLE

Airflow distortion at instrument sites on the RV *Ronald H. Brown*.

REFERENCE

Southampton Oceanography Centre Internal Document, No. 66, 26pp. (Unpublished manuscript)

ABSTRACT

Wind speed measurements obtained from research ships are prone to systematic errors caused by the distortion of the air flow around the ship's hull and superstructure. In this report the air flow around the RV *Ronald H. Brown* is simulated at two relative wind directions using Computational Fluid Dynamics (CFD). The airflow distortion at three anemometer sites has been quantified for wind speed of 15 ms^{-1} blowing a) directly over the bows of the ship, and b) from 30º to port of the bow. All anemometers in this study were located in the bows of the ship and experienced moderate flow distortion, with the wind speed being decelerated by 1% to 4% depending on the instrument location and the wind direction. The flow had been displaced vertically by about 0.7 m for the bow-on flow and by about 0.9 m for the flow from 30º to port.

KEYWORDS

Airflow distortion, R.V. *Ronald H. Brown*, Computational Fluid Dynamics, CFD, wind speed measurement

ISSUING ORGANISATION

Southampton Oceanography Centre
University of Southampton
Waterfront Campus
European Way
Southampton SO14 3ZH
UK **Telephone: 023 8059 6116**

Not generally distributed - please refer to author

AIRFLOW DISTORTION AT INSTRUMENT SITES ON THE R.V. *RONALD H. BROWN*

CONTENTS

AIRFLOW DISTORTION AT INSTRUMENT SITES ON THE R.V. *RONALD H. BROWN*

B. I. Moat, D. I. Berry and M. J. Yelland

January 2001

1. Introduction

This report describes an investigation of the air flow around the R.V. *Ronald H. Brown*. The Computational Fluid Dynamics (CFD) code VECTIS was used to simulate the air flow for two relative wind directions; a) directly over the bows of the ship, and b) 30º off the port bow. Section 2 gives a brief description of the models. The instrument sites examined in this report are those used by researchers from the Woods Hole Oceanographic Institution (WHOI) and the National Oceanic and Atmospheric Administration (NOAA), and are all located above the bows of the ship. The distortion of the air flow at the various instrument sites is examined and percentage wind speed errors are produced for each. The vertical displacement of the flow to each site is also calculated. Section 3 describes the results for the flow directly over the bow, and Section 4 describes those for the flow 30º off the port bow. The results are summarised and discussed in Section 5.

2. The R.V. *Ronald H. Brown* models

The distortion of the airflow at anemometer sites on the *Ronald H. Brown* was determined for an airflow directly over the bow (VECTIS model run 3.4/12) and 30º off the port bow (VECTIS model run 3.4/17). Figure 1 shows the modelled geometry of the R.V. *Ronald H. Brown*. The solid circles indicate the position of the two WHOI "IMET" anemometers and the NOAA sonic anemometer. The co-ordinates of the anemometers for a flow directly over the bow are also shown. The origin of the co-ordinate system is located at the centre of the ship on the "sea surface".

The ship geometry was enclosed in the centre of a "wind tunnel", or computational volume. For flows directly over the bow the computational volume was 600 m long ($-300 < x < 300$), 480 m wide ($-240 < y < 240$) and 150 high ($0 < z < 150$). The centreline of the ship was parallel to the x-axis at $z = 0$. For flows at 30º off the port bow a separate VECTIS model was used. The ship geometry was rotated 30º within the computational volume which was widened to 1200 m to prevent undue blockage of the flow. In both models, a logarithmic wind profile was specified at the inlet of the wind tunnel, with a 10 metre wind speed of 15 ms^{-1}. A parallel 2-processor solver was used to model the flow field. While the computational solver was running the flow in the tunnels was monitored at seven locations towards one side of the tunnel and at one anemometer location, indicated schematically for the bow-on run in Figure 2. Data from the monitoring locations showed that the bow-on solution had converged after about 15800 time steps. Figure 3 shows the velocity of the flow for the last 300 time steps, by which point all values were constant to the third significant figure. The model of the flow 30º over the port bow converged after 21000 time steps. Post-processing files were written for the extraction of data throughout the computational volume. Illustrations of the output are

contained in the Appendix. A complete description of the procedures can be found in Moat *et al.* (1996).

The flow in the tunnels was examined to ensure that free stream conditions existed at the sides and ends of the tunnel, i.e. that the presence of the ship did not cause significant blockage to the flow in the tunnel. As an example, Figure 4a shows the variation of velocity (for the bow-on model) along the tunnel at x = ±250 m, at heights of 10, 20, 30 and 50 m, on a plane at y = 200 m, i.e. towards one side of the tunnel. Equivalent data were also extracted from the opposite side of the tunnel, at y = -200 m, which gave identical results to those shown. The central section of the tunnel is shown in more detail in Figure 4b, which displays velocity data abeam of the ship. This shows a change in free stream velocity of about 0.04 ms^{-1} at 10 m and 0.01 ms^{-1} at a height of 20 m between x = ±50 m. These small changes indicate that the ship caused minimal blockage to the flow at the sides of the tunnel. However, since the changes are not zero, the free stream velocity for a particular instrument site is estimated using the vertical profile of velocity about 200 m directly abeam of the instrument site, rather than the profiles at the inlet or outlet of the tunnel. Examination of the velocity close to the sides of the tunnel for the flow at 30º off the port bow showed that the rotated ship geometry likewise caused minimal blockage to the free stream flow.

3. Results from the bow-on flow model.

3.a The instrument locations

The WHOI IMET instruments were located on the IMET lattice tower situated forwards and to port of the jackstaff mast sited in the bows of the ship (Figure 5). It must be noted that the lattice tower itself was not modelled since its open lattice construction was too fine to be resolved properly in the model. The NOAA sonic anemometer was located on a boom attached to the jackstaff mast which was represented in the model by a cylinder of diameter 0.22 m.

In the VECTIS co-ordinates system, the instrument positions ("P" in Tables 1,2,3) are;

WHOI IMET #1	x = 40.16 m	y = 1.22 m	z (height) = 14.43 m
WHOI IMET #2	x = 40.16 m	y = 1.52 m	z (height) = 14.43 m
NOAA SONIC	x = 41.26 m	y = 0.00 m	z (height) =17.86 m

3.b The vertical displacement of the flow

The vertical displacement of the flow reaching the instruments is found from a streamline traced from the inlet of the tunnel to the instrument site (see Figure A5 in the appendix). Table 1 gives the co-ordinates of; "P" the IMET #1 anemometer site, "P_{stream}" which is the point on the streamline closest to the anemometer, and the position of the start of the streamline "P_{origin}". It can be seen that the streamline is displaced vertically by 0.667 m by the time it reaches the approximate position of the anemometer site. Tables 2 and 3 give the equivalent information for the IMET #2 and NOAA Sonic anemometers respectively. In most cases the streamlines pass within a few centimetres

of the instrument location in the x and z directions, but miss by up to 0.176 m in the y (port-starboard) direction for the IMET #1 anemometer. This is because the streamline originates from a cell far upstream of the ship where the cell size is relatively large. A vertical section (constant y) of data is viewed, and the x and z co-ordinates of the origin of the streamline are adjusted until the streamline passes through the anemometer site, but no such fine adjustment in the y direction is possible. This inaccuracy in the location of the streamlines could cause errors in the calculation of the vertical displacement of up to 10 cm.

Location	x (m)	y (m)	z (m)
P (IMET #1)	40.16	1.22	14.43
P_{stream}	40.157	1.396	14.433
$P-P_{stream}$	0.003	-0.176	0.003
P_{origin}	297.36	1.396	13.766
$P_{stream}-P_{origin}$			$\Delta z=0.667$

Table 1 The vertical displacement, Δz, of the flow to the IMET #1 anemometer.

Location	x (m)	y (m)	z (m)
P (IMET #2)	40.16	1.52	14.43
P_{stream}	40.157	1.396	14.433
$P-P_{stream}$	0.003	0.124	0.003
P_{origin}	297.36	1.396	13.766
$P_{stream}-P_{origin}$			$\Delta z=0.667$

Table 2 The vertical displacement, Δz, of the flow to the IMET #2 anemometer.

Location	x (m)	y (m)	z (m)
P (Sonic)	41.259	0	17.86
P_{stream}	41.264	0.196	17.869
$P-P_{stream}$	-0.005	-0.196	-0.009
P_{origin}	212.35	0.196	17.251
$P_{stream}-P_{origin}$			$\Delta z=0.65$

Table 3 The vertical displacement, Δz, of the flow to the Sonic anemometer.

3.c The free stream velocity

The estimates of the vertical displacement were used to obtain the free stream velocities for the instrument sites. The air parcel reaching the instrument will have originated at a height of $(z-\Delta z)$, and the free stream velocity is obtained at that height on the free stream profile. The velocity of the flow at the instrument site is then compared to this free stream velocity to give the wind speed error.

Figure 6 shows part of the free stream profile near the wind tunnel wall, directly abeam of the IMET #1 anemometer ($x = 40.16$, $y = 200$, $0 < z < 200$). This indicates a free stream velocity of

15.531 ms^{-1} at a height of 13.763 m. Free stream velocities were obtained for the other instruments sites in a similar fashion and are shown in Table 4.

3.d The effect of flow distortion on the wind speed.

The free stream flow has small, predictable gradients and can be estimated accurately at any given point on the vertical profile. In contrast, the flow at an instrument site can suffer from severe distortion and correspondingly large gradients in the velocity field. In addition, it is not always possible to locate the centre of a computational cell on the exact instrument position (see Section 3.b and Moat *et al.*, 1996). For these reasons the velocity at the instrument site is estimated from lines of data extracted in all three directions. Figures 7 to 9 show the lines of data through the IMET #1, IMET #2 and NOAA sonic positions respectively. The results for the instruments are summarised in Table 4. The velocity error at the instrument site (of height z) is expressed as a percentage of the free stream velocity (at height z-Δz). A positive error indicates that the flow at the instrument site has been accelerated.

Figures 7 to 9 are also used to estimate the gradient of the velocity of the flow in all three directions. These rates of change of velocity provide an indication of the accuracy of the velocity error estimate and of the severity of the local flow distortion. The rates of change for all the instruments are given in terms of change per cell and change per metre in Table 5. Unlike the NOAA site, the results for the IMET sites show significant rates of change in the horizontal which suggests that these sites are affected to some degree by the presence of the jackstaff mast. This can be seen in Figures 7a, 8a and 9b. In general the effects of flow distortion at all three sites is moderate, with the flow being displaced vertically by less than one metre and decelerated by 3 to 4 %. This is confirmed by the angle of the flow to the horizontal; the wind speed components suggest an angle of flow to the horizontal of about 3.7º for IMET #1, 4.0º for IMET #2, and 2.8º for the NOAA sonic.

Instrument site	Velocity from Each direction	Average velocity (ms^{-1})	Free stream velocity (ms^{-1})	% Error
IMET #1	14.965 (x)	14.967	15.531	-3.63
	14.971 (y)			
	14.965 (z)			
IMET #2	14.831 (x)	15.008	15.531	-3.37
	15.010 (y)			
	15.006 (z)			
NOAA sonic	15.282 (x)	15.298	15.887	-3.70
	15.282 (y)			
	15.331 (z)			

Table 4 Wind speed errors at the instrument sites (bow-on flow).

Instrument site	Velocity data line	Rate of change of velocity per metre (ms^{-1}/m)	Rate of change of velocity per cell (ms^{-1}/cell)
IMET #1	along (x)	0.148	0.037
	across (y)	0.229	0.018
	up (z)	0.134	0.021
IMET #2	along (x)	0.152	0.040
	across (y)	0.162	0.010
	up (z)	0.131	0.020
NOAA sonic	along (x)	0.078	0.024
	across (y)	0.005	0.004
	up (z)	0.142	0.096

Table 5 Rate of change of velocity close to the anemometer sites (bow-on flow).

4. Results for a flow 30º off the port bow.

4.a The instrument locations

The procedures used for this model were the same as those described in Section 3.

In the VECTIS co-ordinates system, the instrument positions ("P" in Tables 6,7,8) are;

WHOI IMET #1	x = 35.39m	y = -19.02m	z (height) = 14.43 m
WHOI IMET #2	x = 35.54m	y = -18.76m	z (height) = 14.43 m
NOAA SONIC	x = 35.75m	y = -20.63m	z (height) = 17.86 m

4.b Vertical displacement and velocity error

Tables 6, 7 and 8 show the vertical displacement of the flow reaching the three anemometers. Figures 10 to 12 show the velocity data extracted at the anemometer locations, and the resulting errors in the velocities are shown in Table 9. Table 10 gives the rates of change of the velocity errors.

Location	x (m)	y (m)	z (m)
P (IMET #1)	35.39	-19.02	14.43
P_{stream}	35.392	-19.218	14.434
$P-P_{stream}$	-0.002	0.198	-0.004
P_{origin}	299.08	-19.218	13.583
$P_{steam}-P_{origin}$			$\Delta z = 0.851$

Table 6 The vertical displacement, Δz, of the flow to the IMET#1 anemometer (flow 30º to port)

Location	x (m)	y (m)	z (m)
P (IMET #2)	35.54	-18.76	14.43
P_{stream}	35.540	-18.738	14.433
$P-P_{stream}$	0	-0.022	-0.003
P_{origin}	299.06	-18.738	13.552
$P_{steam}-P_{origin}$			$\Delta z = 0.881$

Table 7 The vertical displacement, Δz, of the flow to the IMET#2 anemometer (flow 30º to port)

Location	x (m)	y (m)	z (m)
P (NOAA Sonic)	35.73	-20.63	17.86
P_{stream}	35.75	-20.533	17.837
$P-P_{stream}$	-0.02	-0.097	0.023
P_{origin}	233.39	-20.533	16.997
$P_{steam}-P_{origin}$			$\Delta z = 0.840$

Table 8 The vertical displacement, Δz, of the flow to the NOAA Sonic anemometer (flow 30º to port)

Instrument site	Velocity from Each direction	Average velocity (ms^{-1})	Free stream velocity (ms^{-1})	% Error
IMET#1	14.799 (x) 14.952 (y) 14.937 (z)	14.896	15.404	-3.30
IMET #2	15.031 (x) 15.043 (y) 15.024 (z)	15.033	15.399	-2.38
NOAA sonic	15.556 (x) 15.568 (y) 15.563 (z)	15.562	15.730	-1.07

Table 9 Percentage error at the instrument sites (flow 30º to port).

Instrument site	Velocity data line	Rate of change of velocity per metre (ms^{-1}/m)	Rate of change of velocity per cell (ms^{-1}/cell)
IMET #1	along (x)	0.278	0.079
	across (y)	0.091	0.034
	up (z)	0.099	0.019
IMET #2	along (x)	0.019	0.016
	across (y)	0.117	0.028
	up (z)	0.099	0.019
NOAA sonic	along (x)	0.009	0.006
	across (y)	0.210	0.029
	up (z)	0.119	0.035

Table 10 Rate of change of velocity close to the anemometer sites (flow 30º to port).

The vertical displacement of the flow at all sites was between 0.8 and 0.9 m, larger than that found for the bow-on flow. This is to be expected since the forward part of the ship's hull presents a larger obstacle when at an angle to the flow than when bow-on. This increase in the distortion to the flow is also reflected in the larger angles to the horizontal made by the mean flow; 5.6º for IMET #1, 5.0º for IMET #2, and 3.4º for the NOAA sonic. The wind speed errors are slightly less than for the bow-on flow, especially at the NOAA site where the flow was decelerated by just over 1% compared to a deceleration of nearly 4% for the bow-on flow.

5. Summary

The distortion of the airflow at three anemometer sites on the R.V. *Ronald H. Brown* has been quantified for a 10 m wind speed of 15 ms^{-1} blowing a) directly over the bows of the ship, and b) from 30º to port of the bow. The distortion of the simulated flow is due to the ship's hull and superstructure only, since small scale structures (the structure of the lattice tower) and very local obstructions (the other instruments) could not be modelled.

The vertical displacement (Δz) of the flow was used to obtain an effective anemometer height ($z-\Delta z$), and the wind speed error relates the actual flow at the instrument site to the free stream flow at this effective height. The effective height and the correct wind speed relative to this height are required if the data from the anemometer is used to calculate the wind stress via the dissipation method (Yelland *et al.*, 1998). The results for both models and all three instrument sites are summarised in Table 11. If the actual (rather than the effective) height of the instrument is used to obtain the free stream velocity then the wind speed error at the instrument site will change accordingly. Table 12 shows the results for each instrument if the free stream velocity is calculated in this fashion. Since the vertical displacement of the flow was less than 1 m in all cases the change in the wind speed error is small, being about 0.3% for the bow-on flow and 0.7% for the flow at 30º to port.

Instrument (Run angle)	Instrument height z (m)	Velocity at instrument site (ms^{-1})	Free stream velocity (at $z - \Delta z$) (ms^{-1})	% velocity error at instrument site	Vertical displacement Δz (m)	Angle of flow to the horizontal (degrees)
Flow directly over the bow						
IMET #1 (0º)	14.43	14.967	15.531	**-3.63 (0.2)**	**0.67±0.1**	**3.7**
IMET #2 (0º)	14.43	15.008	15.531	**-3.37 (0.3)**	**0.67±0.1**	**4.0**
NOAA sonic (0º)	17.86	15.298	15.887	**-3.70 (0.6)**	**0.65±0.1**	**2.8**
Flow 30º off the port bow						
IMET #1 (30º)	14.43	14.896	15.404	**-3.30 (0.5)**	**0.85±0.1**	**5.6**
IMET #2 (30º)	14.43	15.033	15.399	**-2.38 (0.2)**	**0.88±0.1**	**5.0**
NOAA sonic (30º)	17.86	15.562	15.730	**-1.07 (0.2)**	**0.84±0.1**	**3.4**

Table 11 Summary of the results for all instrument sites on the R.V. *Ronald H. Brown*. The figures in brackets indicate the maximum rate of change of velocity per cell (expressed as a percentage of the free stream velocity) for each site.

The vertical displacement of the flow is due to the large structure of the ship's hull and is relatively insensitive to the exact instrument location, with very similar displacements at all sites despite their physical separation of up to 4 m. The effect of the distortion on the velocity is rather more dependent on the instruments position since the speed of the flow is affected the smaller structure of the jackstaff mast as well as the large structure of the hull.

The greatest source of error in the results is likely to be in the extraction of the data. For the bow-on flow, Table 5 shows that the maximum variation of the velocity from one cell to the next in the location of the instruments is 0.037 ms^{-1}/cell for the IMET #1, 0.040 ms^{-1}/cell for the IMET #2 and 0.096 ms^{-1}/cell for the NOAA Sonic. These values, along with those for the 30º flow, are expressed as a percentage of the free stream flow and are shown in brackets in Table 11. For both model runs and all instrument sites, the largest uncertainty in the velocity error is about 0.5%. However, the IMET instruments are fairly close to the jackstaff mast (1.5 m and 1.8 m for instruments 1 and 2 respectively), and are on the edge of the region which experiences local flow distortion caused by the mast (Figures 7a, 8a and 9b). The model used a mast diameter of 0.22 m which was estimated from the general arrangement plans of the ship, and the results could be affected if this differs significantly from the actual dimension.

Overall, the anemometer sites experience only moderate flow distortion, with the wind speed being decelerated by less than 4% and displaced vertically by less than a metre. However, the results differ significantly for the two different wind direction: this is to be expected since the ship presents a larger obstruction when at an angle to the flow than when the flow is over the bows.

General information about the CFD work and more images of the *Ronald H. Brown* models can be found at http://www.soc.soton.ac.uk/JRD/MET/cfd_shipflow.php3.

Instrument	Instrument Height, z. (m)	Velocity at instrument (ms^{-1})	Free stream velocity at height z (ms^{-1})	% velocity error at instrument site
Flow directly over the bow				
IMET #1 (0º)	14.43	14.967	15.588	-3.98
IMET #2 (0º)	14.43	15.008	15.588	-3.72
NOAA sonic (0º)	17.86	15.298	15.930	-3.97
Flow 30º off the port bow				
IMET #1 (30º)	14.43	14.896	15.524	-4.05
IMET #2 (30º)	14.43	15.033	15.524	-3.16
NOAA sonic (30º)	17.86	15.562	15.832	-1.70

Table 12 The wind speed errors calculated using a free stream velocity at the actual instrument height, z.

6. Acknowledgments

This work was supported by funds from the Woods Hole Oceanographic Institute.

7. References

Moat, B. I., Yelland, M. J., and Hutchings, J.: 1996, 'Airflow over the R.R.S. Discovery using the Computational Fluid Dynamics package VECTIS', SOC Internal Report No. 2, Southampton Oceanography Centre, Southampton, UK.

Yelland, M. J., Moat, B. I., Taylor, P. K., Pascal, R. W., Hutchings, J., and Cornell, V. C.: 1998, 'Wind stress measurements from the open ocean corrected for air-flow distortion by the ship', *Journal of Physical Oceanography* **28**, 1511 - 1526.

8. Figures

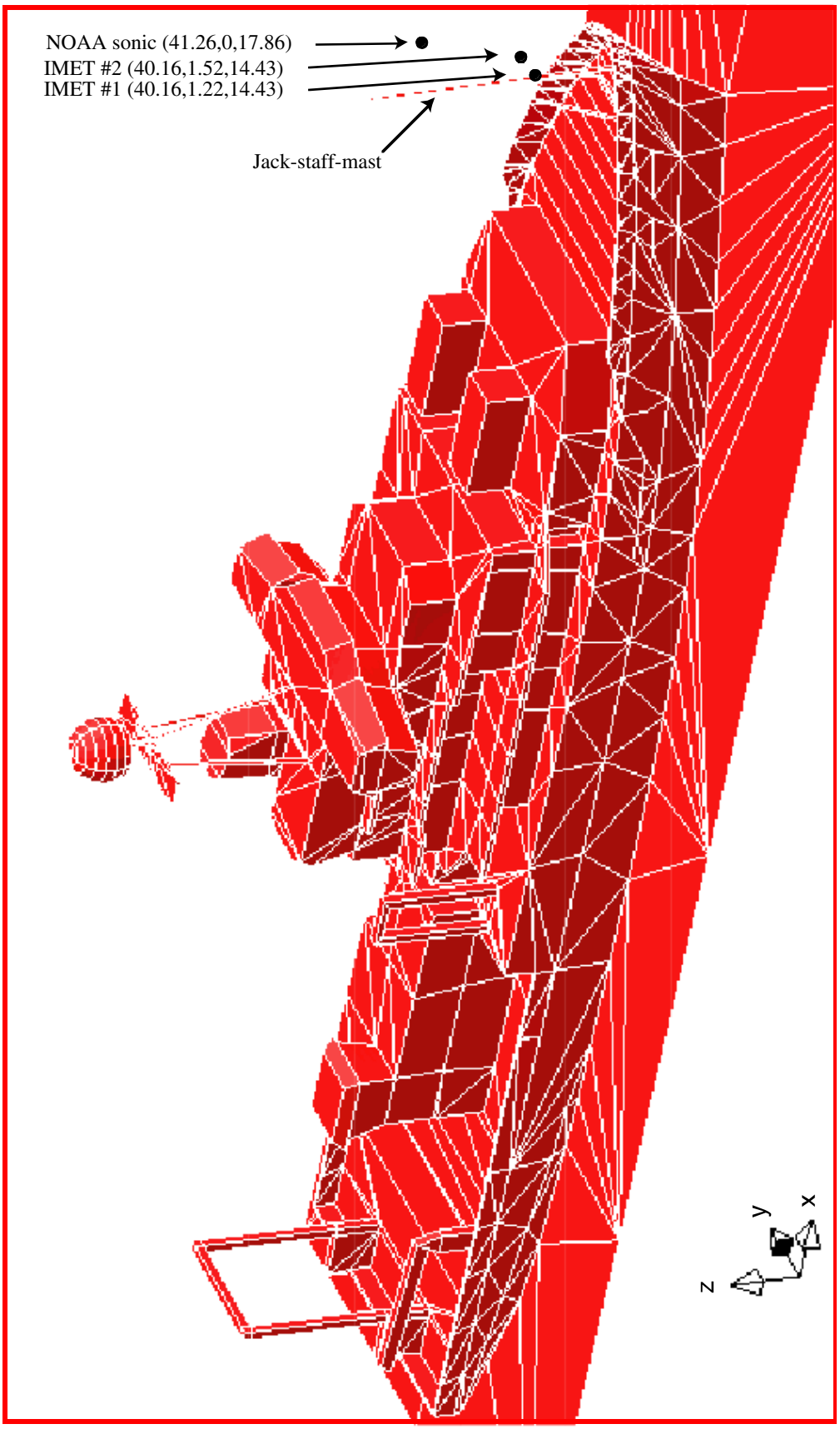

Figure 1 A 3-dimensional view of the model of the RV *Ronald H. Brown*.

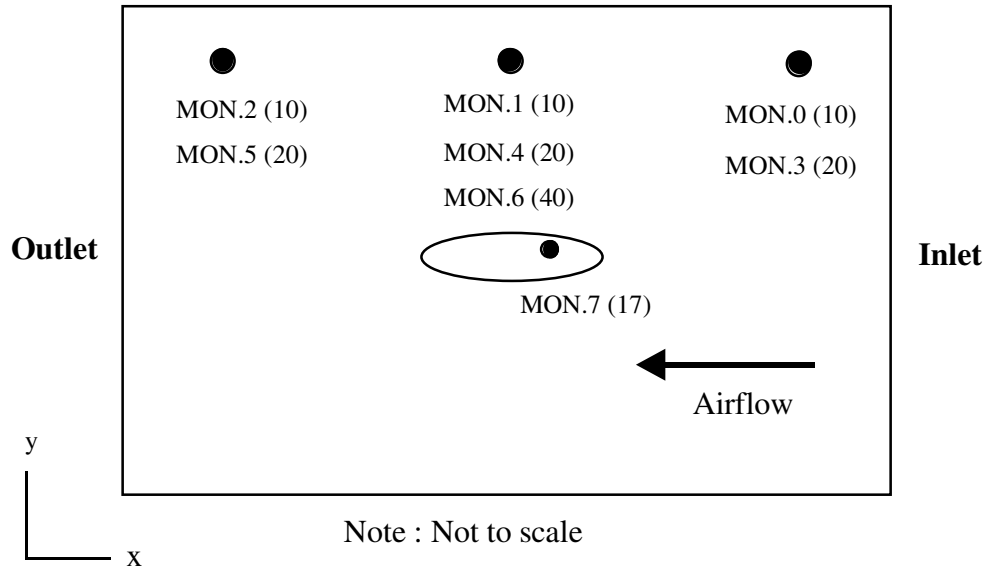

Figure 2. Schematic plan view of the wind tunnel used to simulate a flow of air over the bows of the R.V. *Ronald H. Brown*. The monitoring positions are shown by the solid circles and their heights in metres are indicated in brackets.

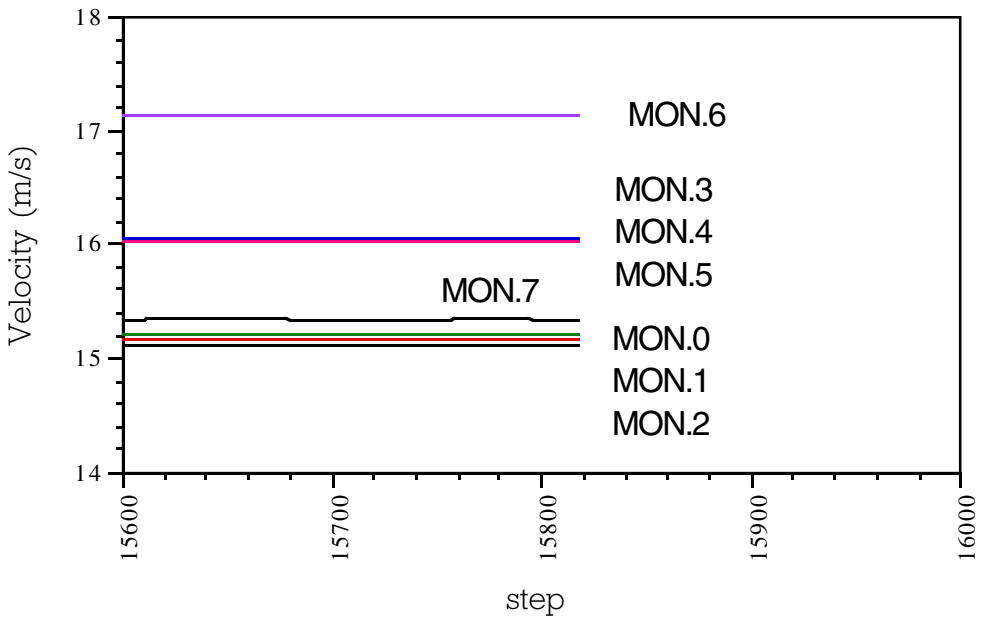

Figure 3 Velocity data from the eight monitoring locations, for the last 300 time steps.

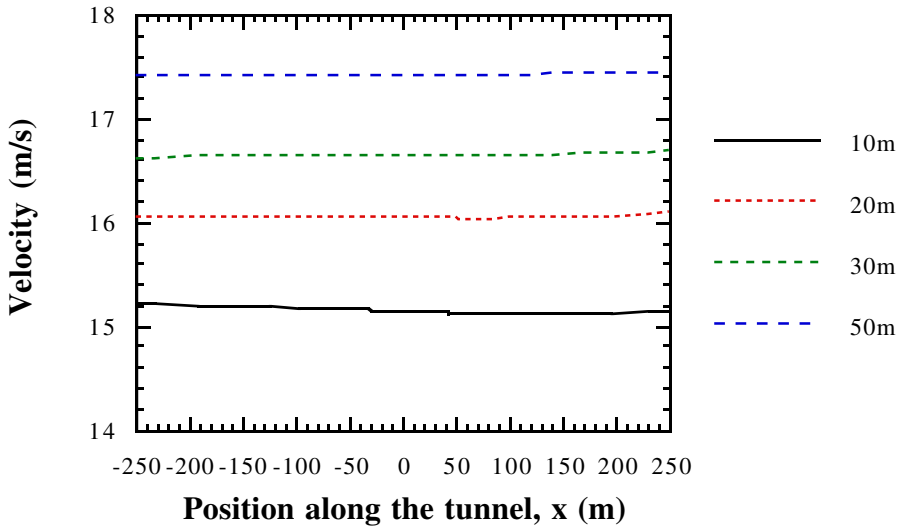

Figure 4a. Lines of velocity data along the length of the tunnel at the heights shown. The data were obtained from the free stream region towards one side of the tunnel.

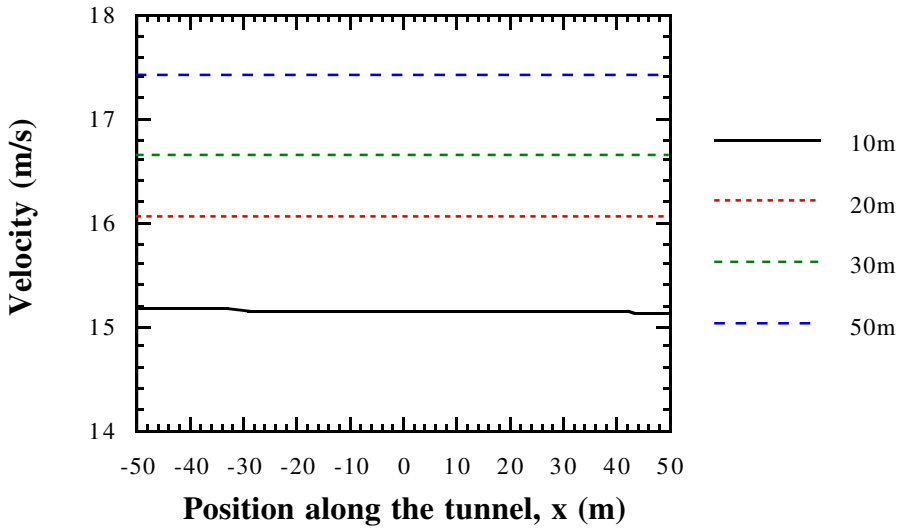

Figure 4b. As 4a, showing the central portion of the tunnel only.

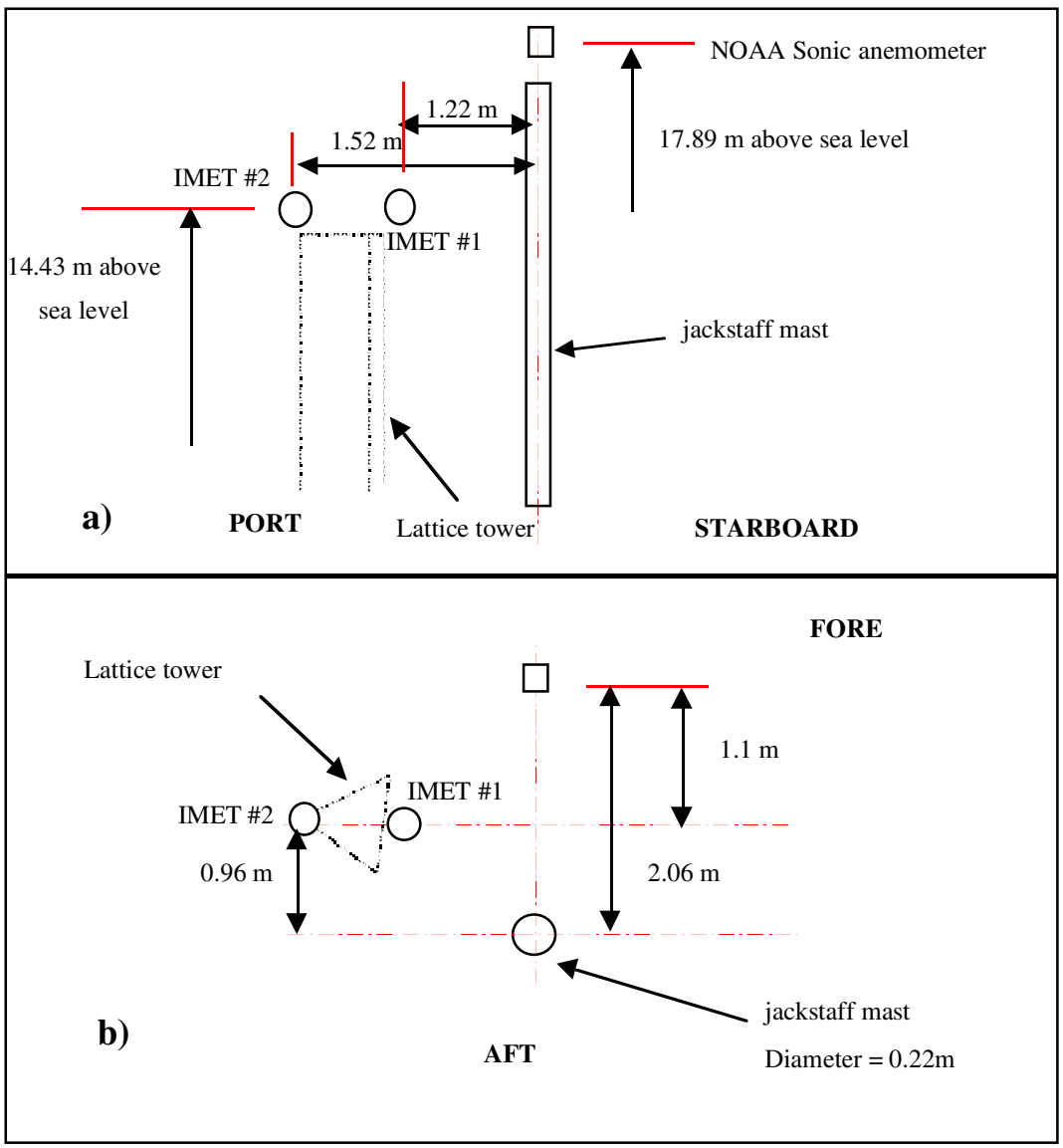

Figure 5 Schematic of the instrument positions relative to the lattice tower and jackstaff mast in the bows of the R.V. *Ronald H. Brown*; a) viewed from astern and b) plan view. The jackstaff mast is represented by a cylinder of diameter 0.22 m. N.B. The lattice tower itself is not modelled.

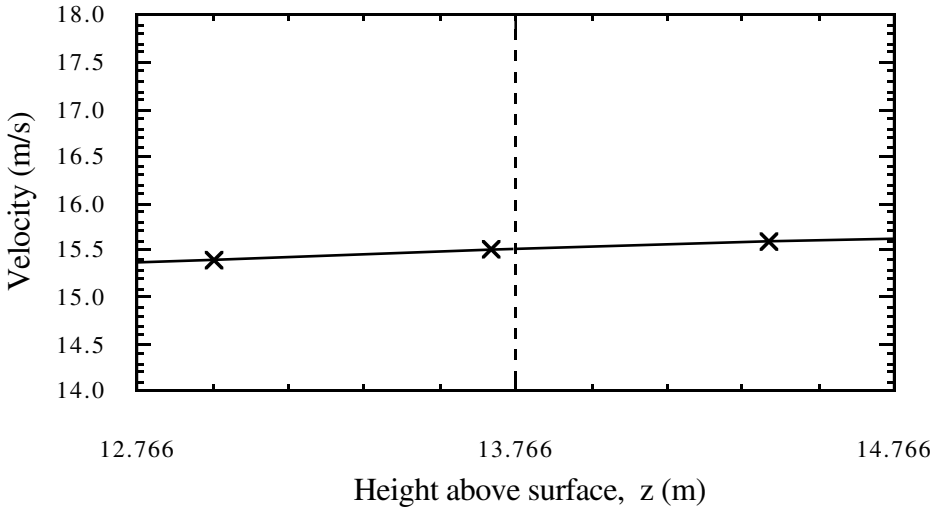

Figure 6 The vertical profile of velocity abeam of the IMET #1 anemometer site. The dashed line indicates the height at which the air flow originated.

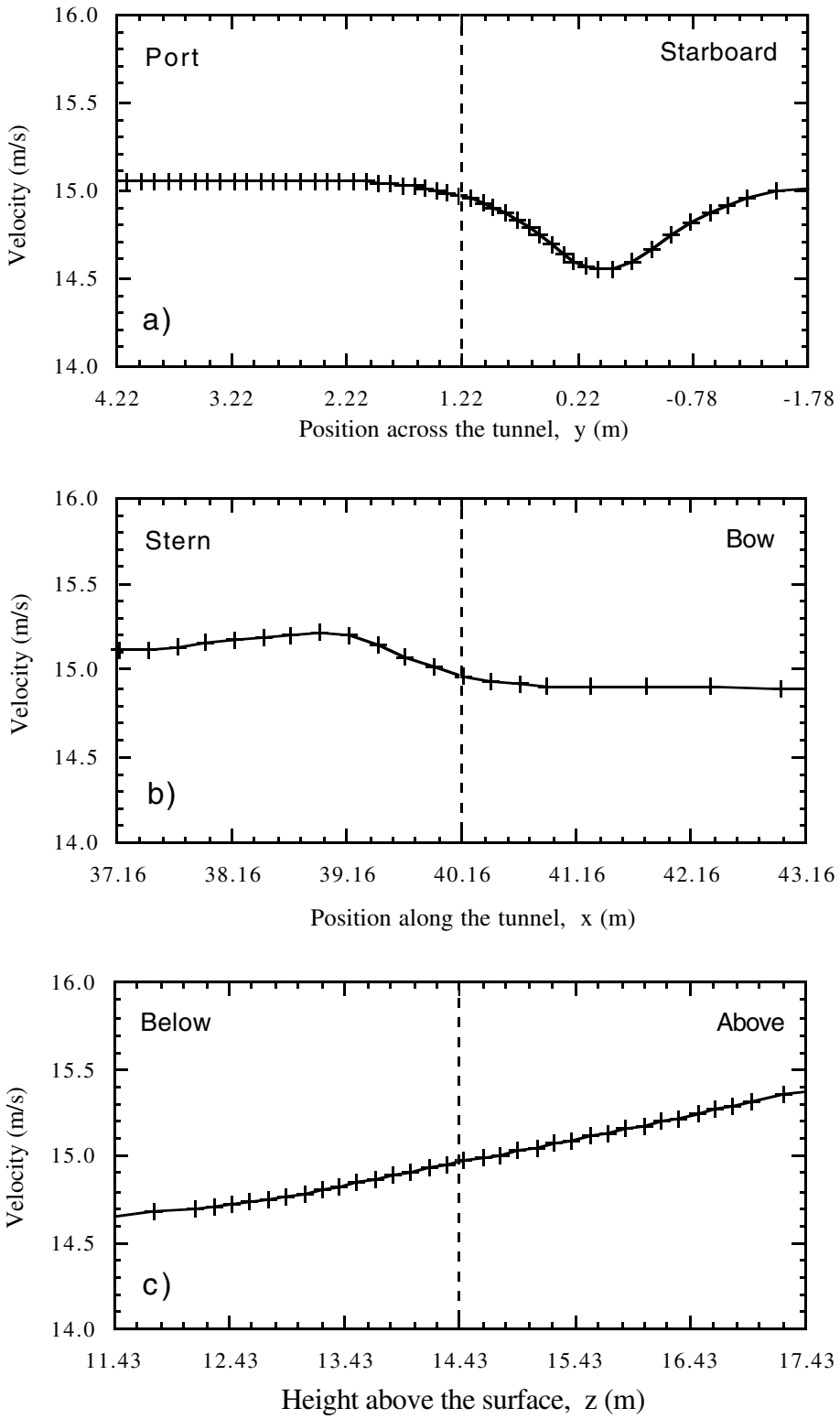

Figure 7 Lines of velocity data through the IMET #1 position (indicated by the dashed line) in all three directions; a) across the tunnel (y), b) along the tunnel (x) and c) vertically (z). Results are from the model of a bow-on flow.

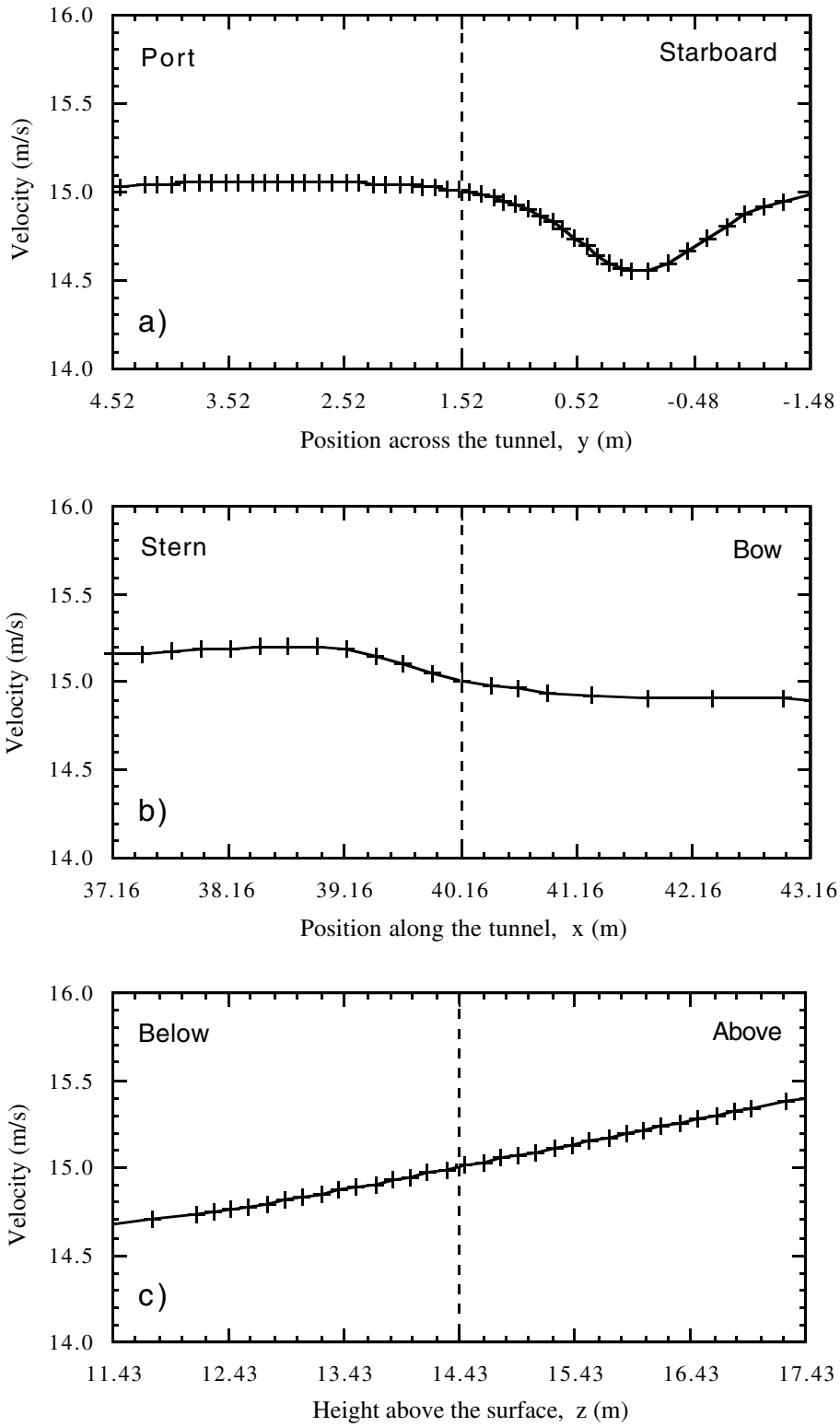

Figure 8 As for Figure 7, but for the IMET #2 anemometer site.

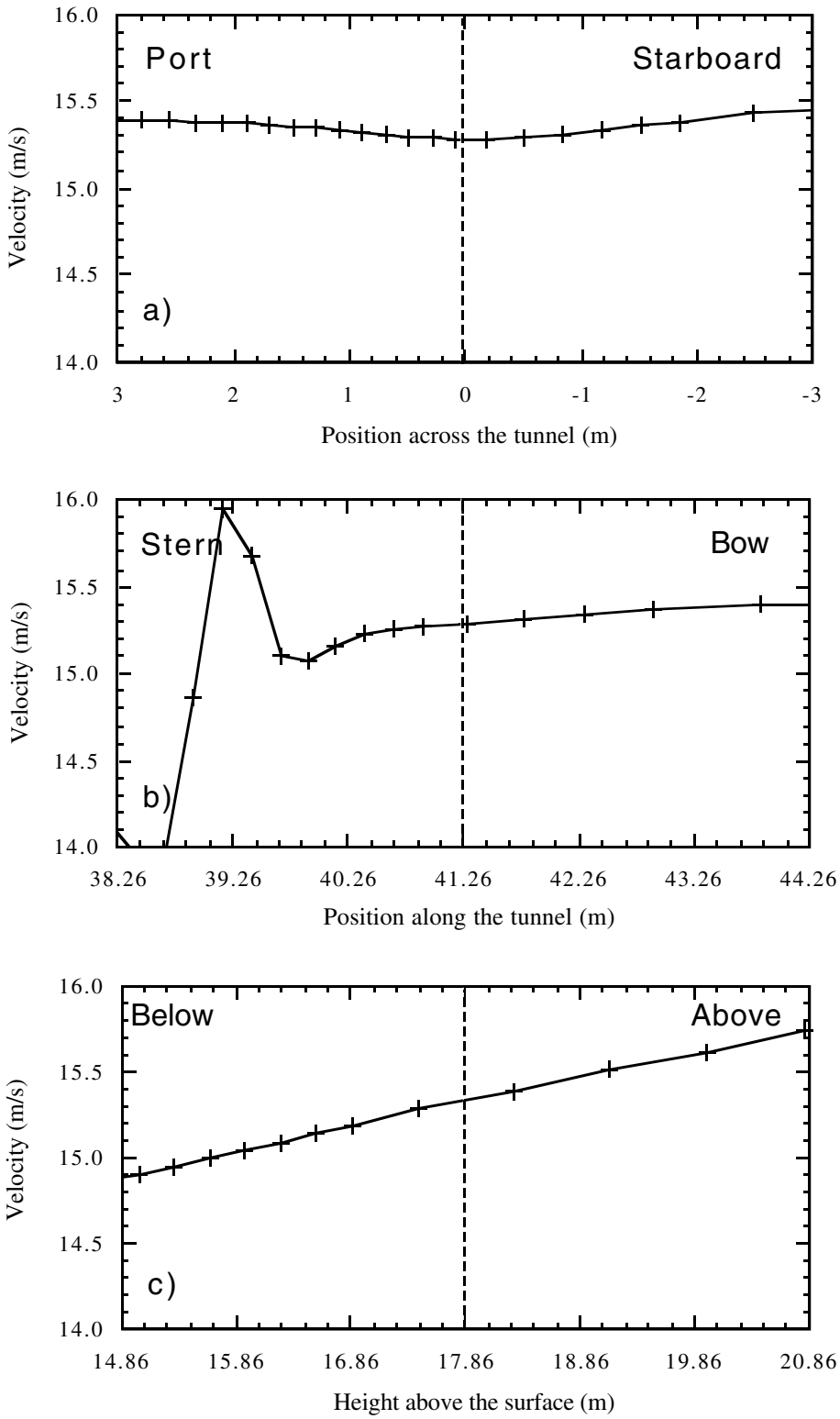

Figure 9 As for Figure 7, but for the NOAA sonic anemometer site.

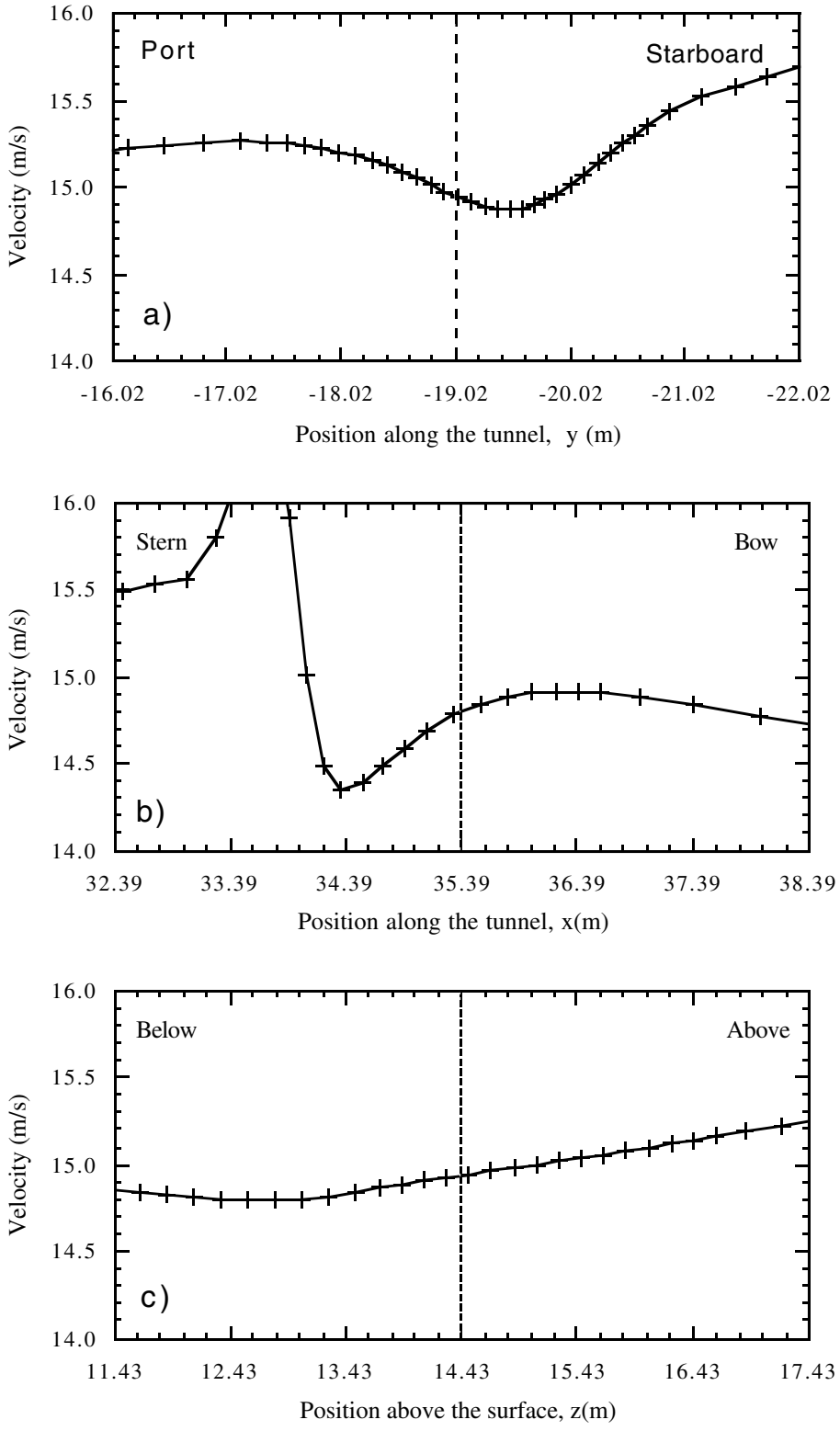

Figure 10 As for Figure 7, but for the IMET #1 anemometer site modelled for a flow at 30º off the port bow.

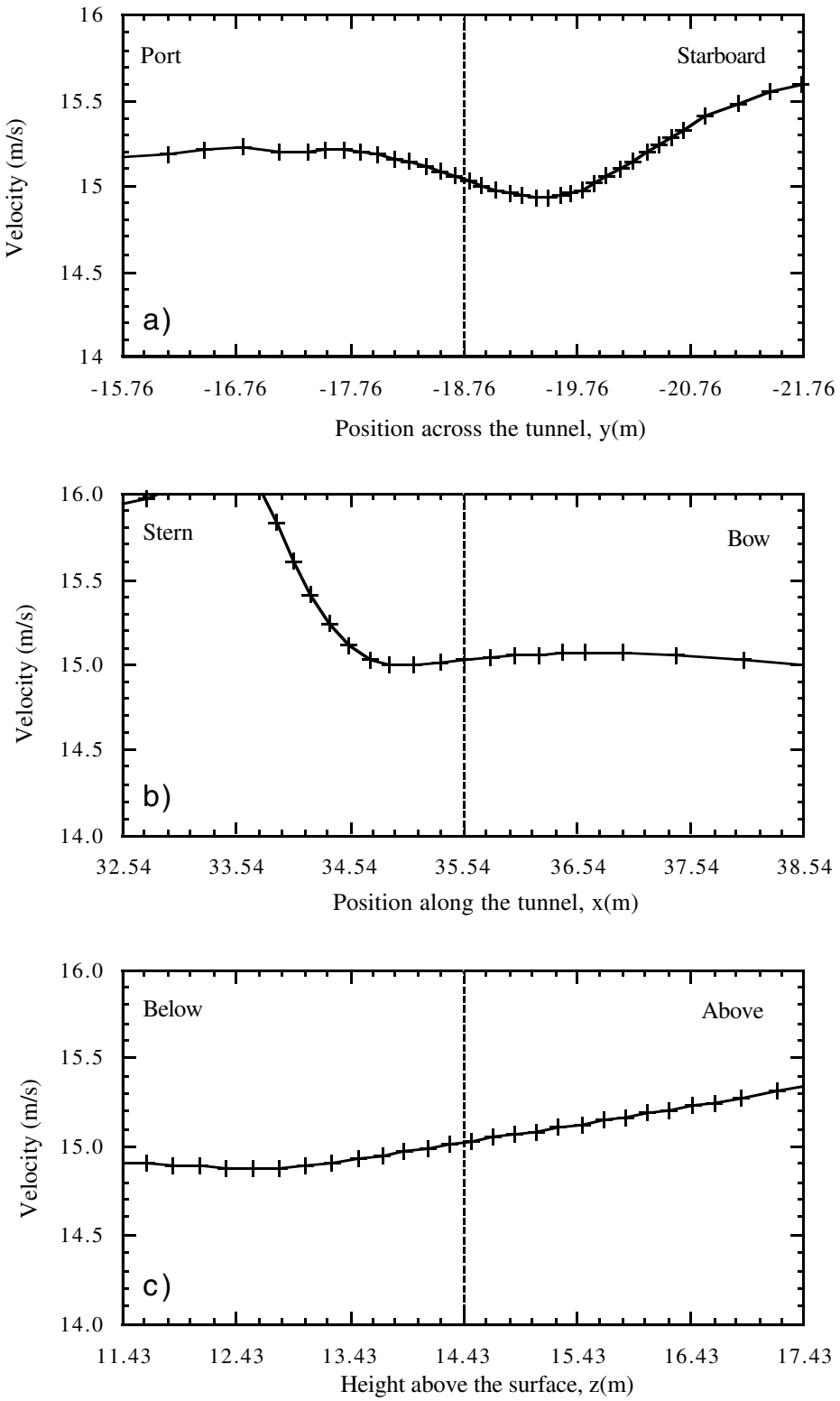

Figure 11 As for Figure 7, but for the IMET #2 anemometer site modelled for a flow at 30º off the port bow.

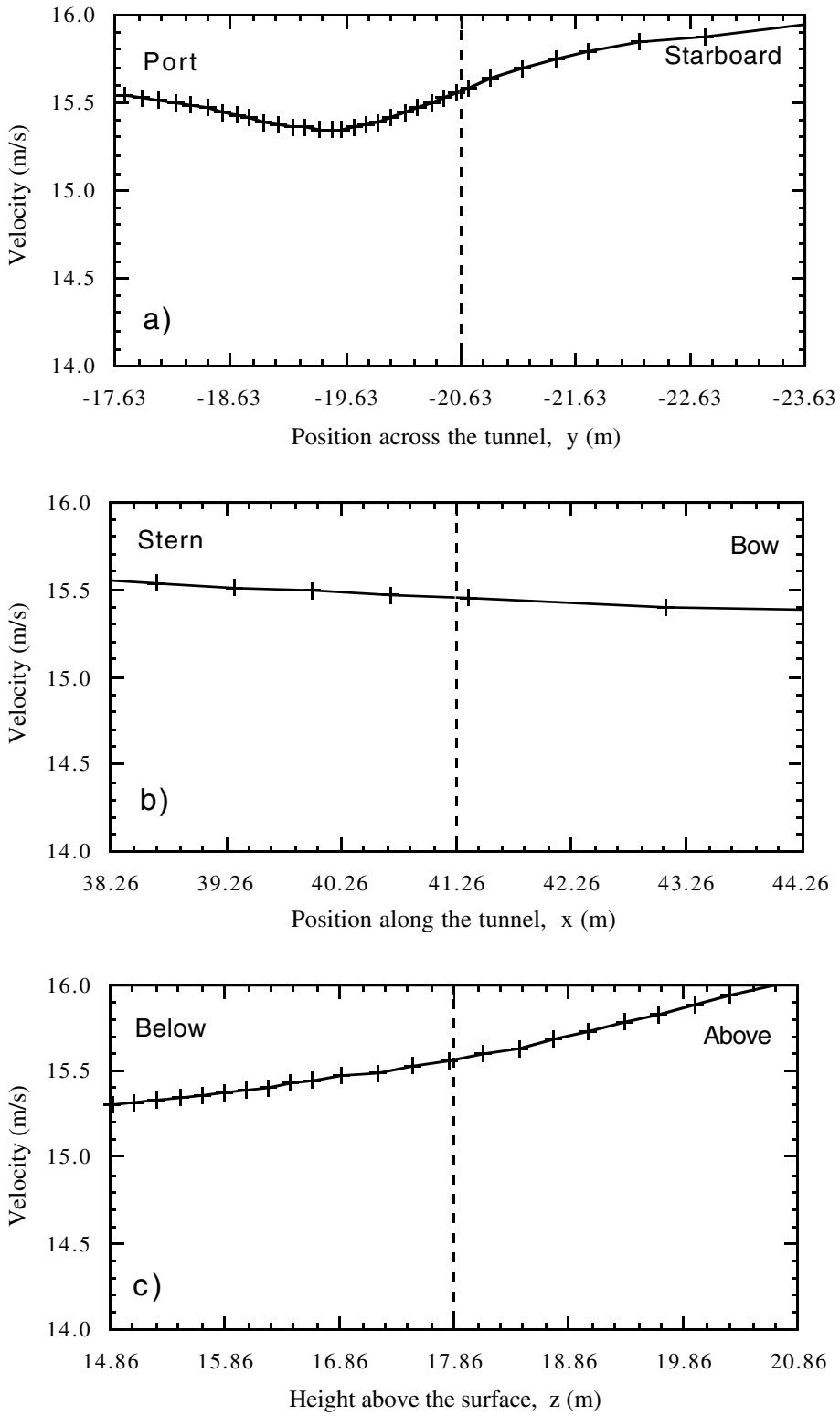

Figure 12 As for Figure 7, but for the Sonic anemometer site modelled for a flow at 30° off the port bow.

9. Appendix

The Figures in this Appendix were generated using the VECTIS post-processing software. Each Figure shows data on a major plane, and the orientation of the plane is indicated by a red line in the small box at the top left of each Figure. The variable size of the computational cells can be seen in all the Figures.

Figure A1 Velocity vectors on a vertical plane through the IMET instrument sites. The magnitude of the total velocity is indicated by the colour of the arrows. The length and direction of the arrows represent the magnitude and direction of the component of the velocity in the plane of view. Each arrow represents the result from one computational cell. The velocity scale corresponds to 13 ms^{-1} to 18 ms^{-1}. The position of the IMET instruments are indicated by the crosses.

FIGURE A2 As Figure A1 for a vertical plane through the NOAA sonic anemometer site (indicated by the cross).

FIGURE A3 As Figure A1 for a vertical section across the tunnel which intersects the IMET instrument sites (indicated by the crosses).

FIGURE A4 As Figure A1 for a horizontal section through the IMET instrument sites (indicated by the crosses).

FIGURE A5 A streamline, or massless particle trace, which passes through the NOAA anemometer site (indicated by the cross).

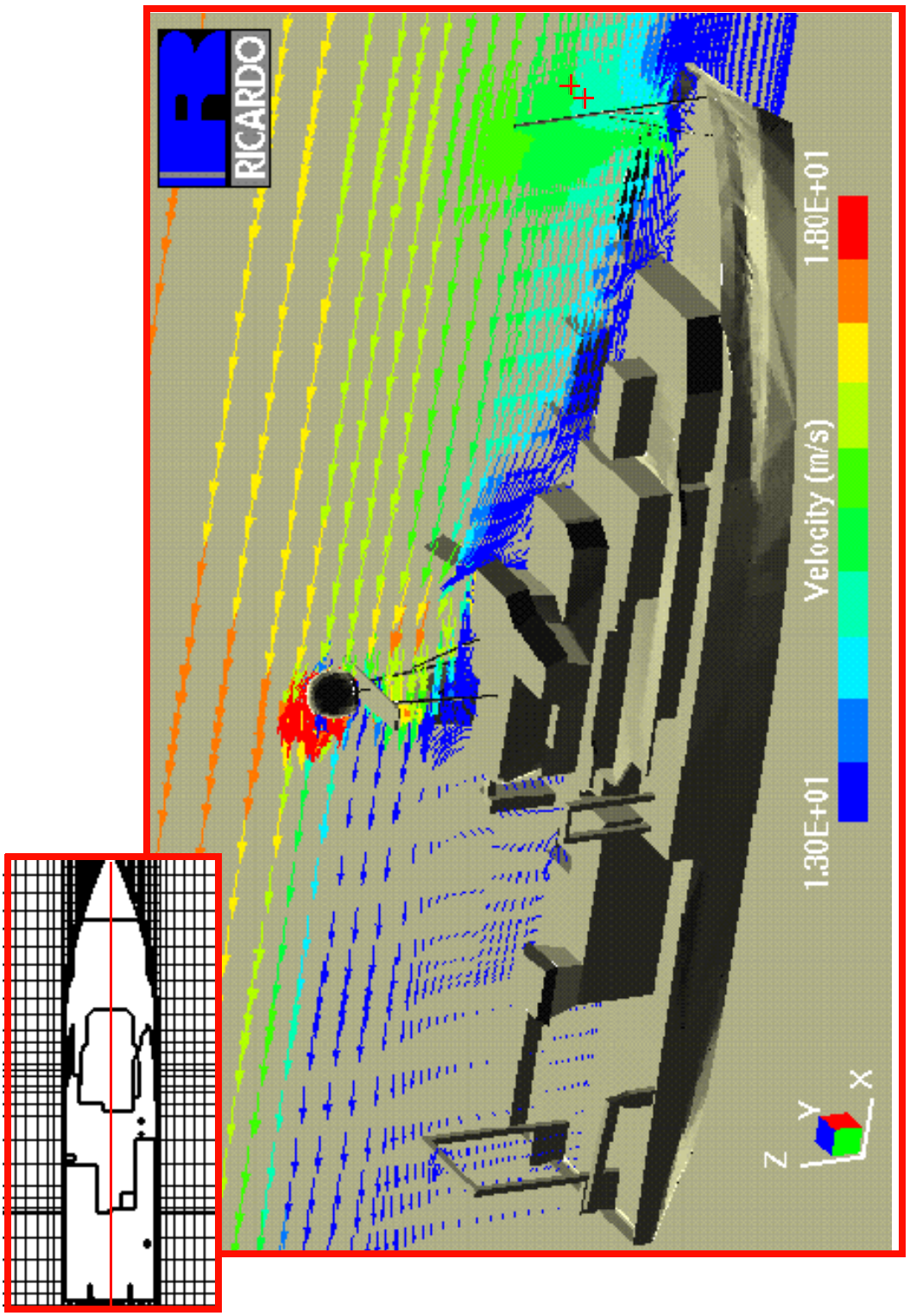

Figure A1

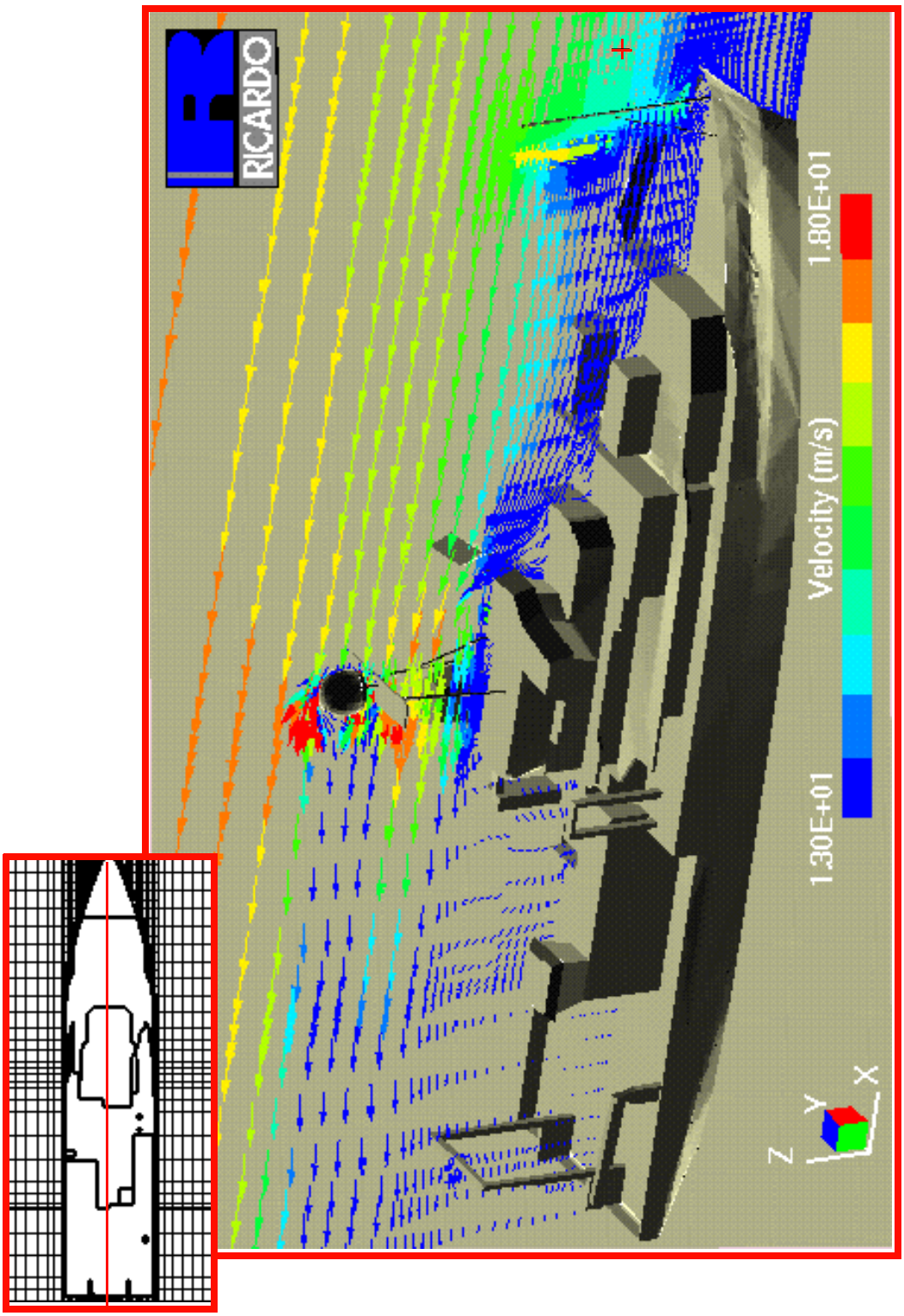

Figure A2

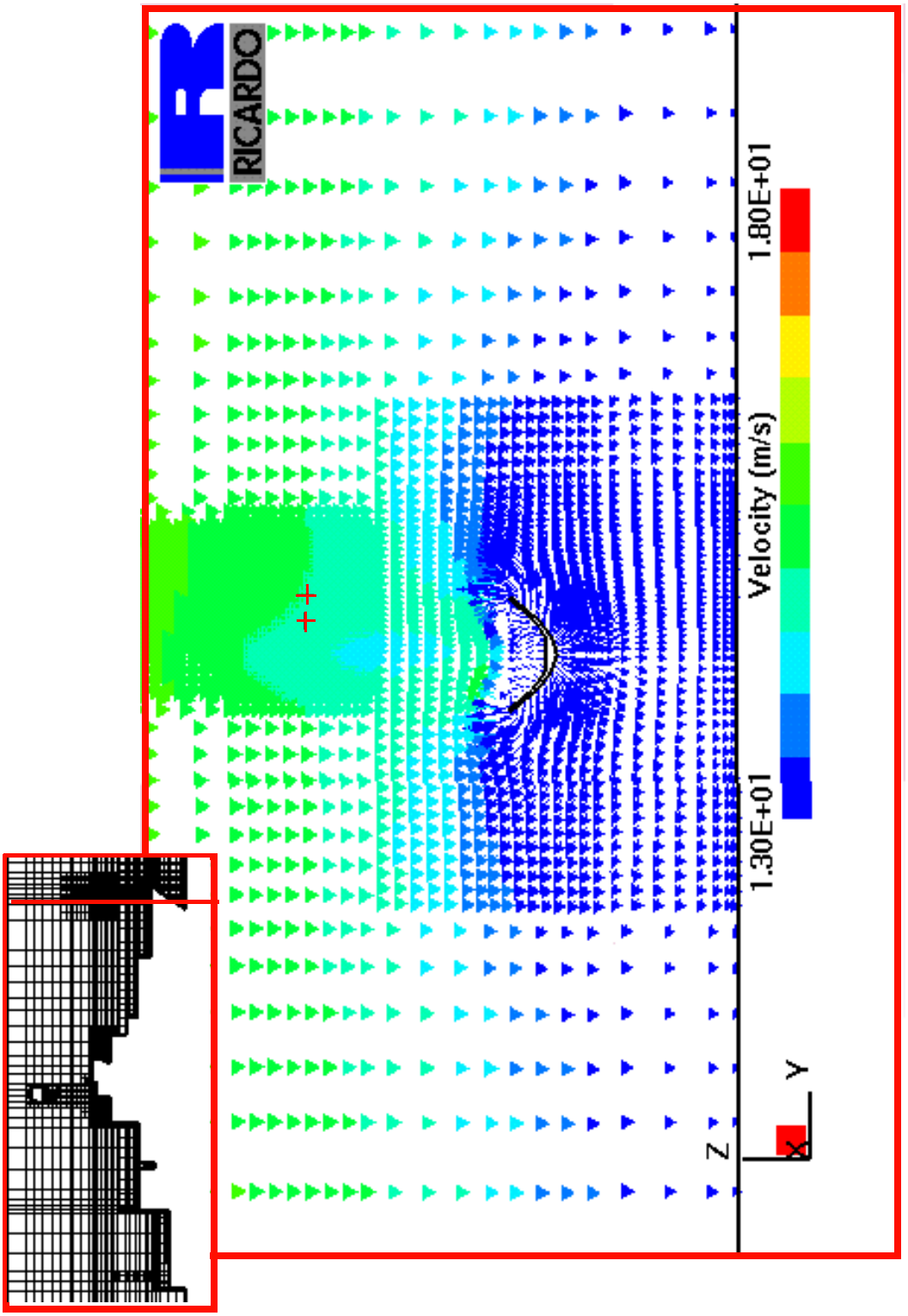

Figure A3

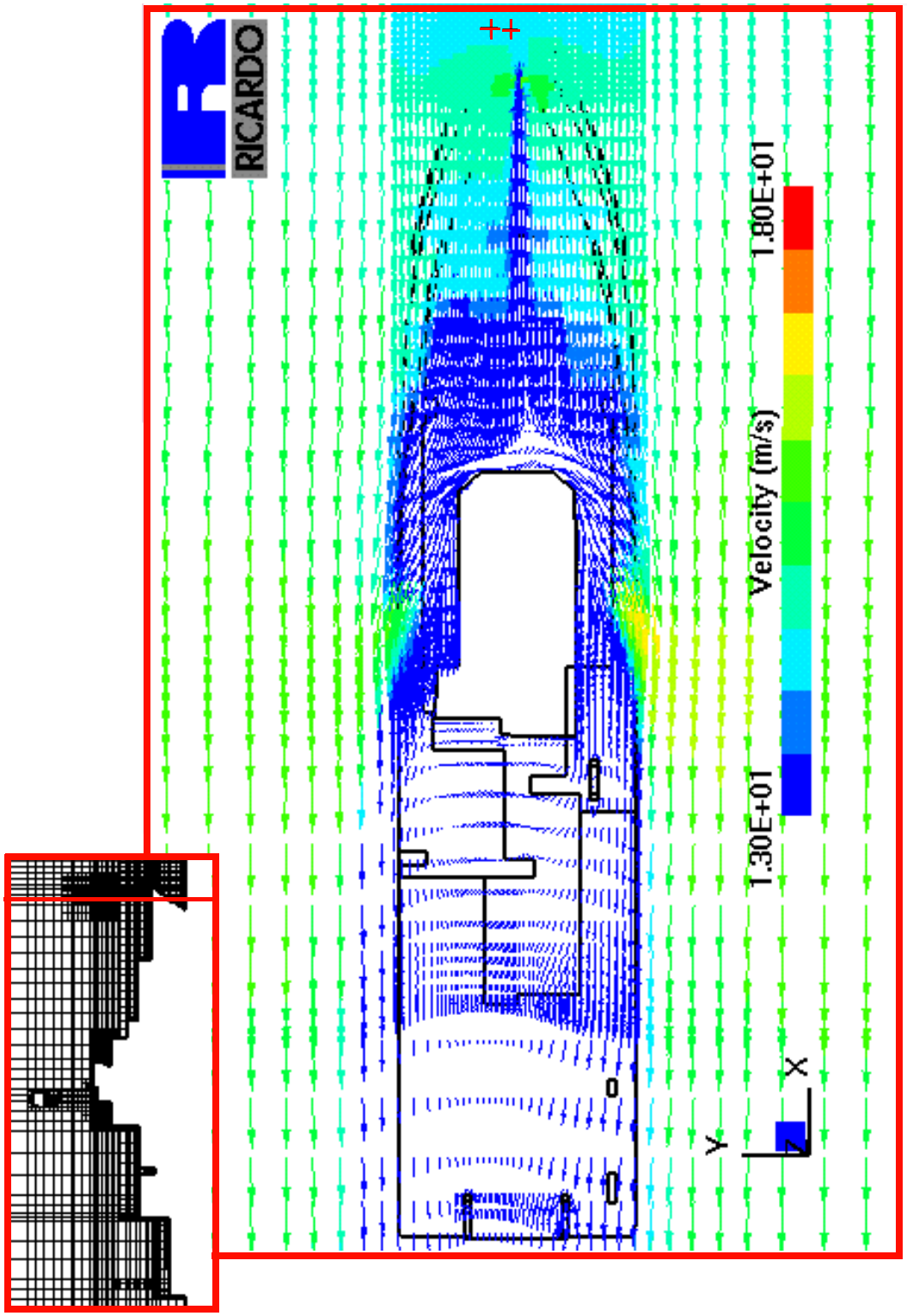

Figure A4

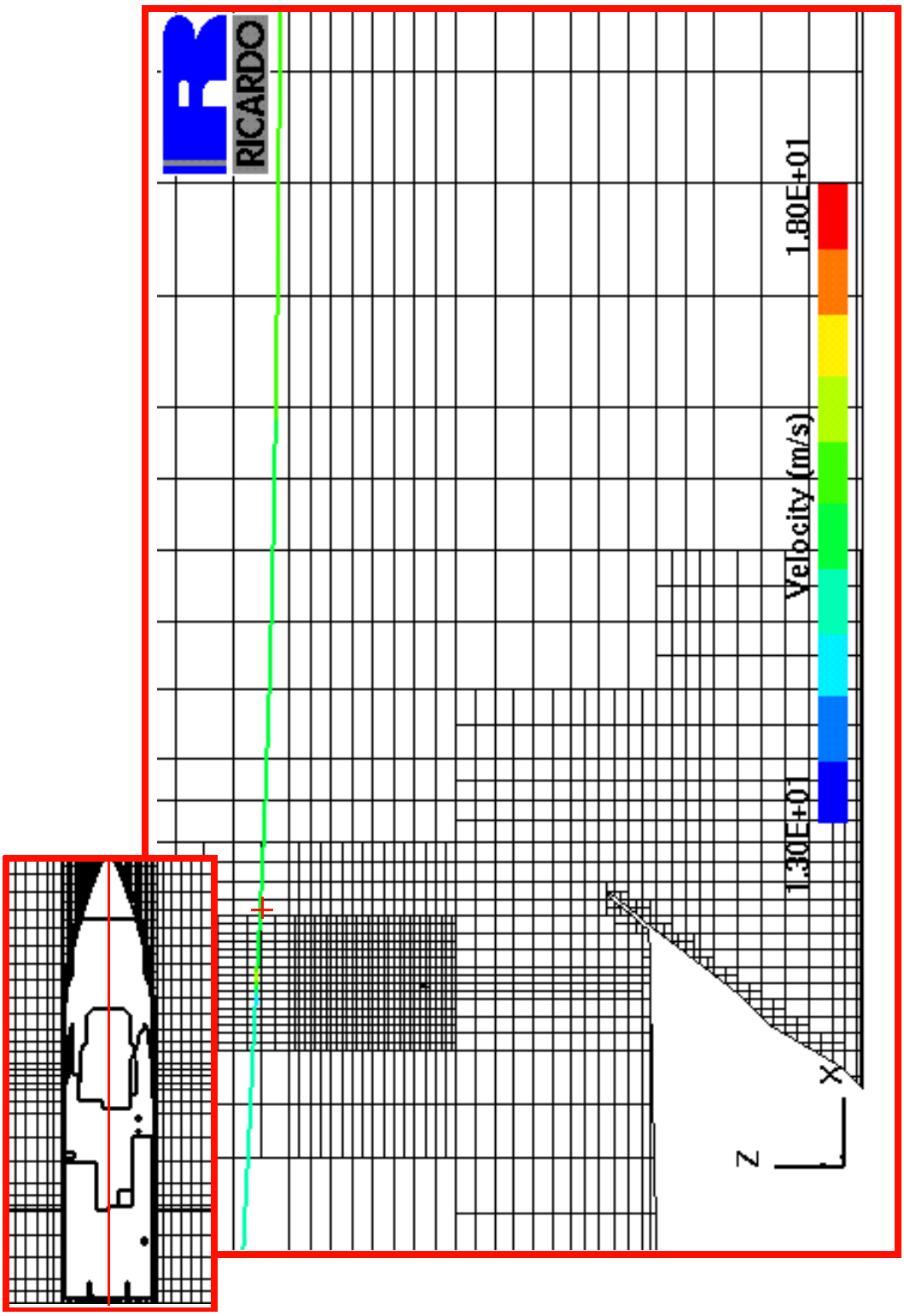

Figure A5